Article

Molecular Containers Based on Amphiphilic PS-*b*-PMVE Dendrigraft Copolymers: Topology, Organization, and Aqueous Solution Properties

Michel Schappacher, Jean Luc Putaux, Christelle Lefebvre, and Alain Deffieux

J. Am. Chem. Soc., **2005**, 127 (9), 2990-2998• DOI: 10.1021/ja0440203 • Publication Date (Web): 08 February 2005

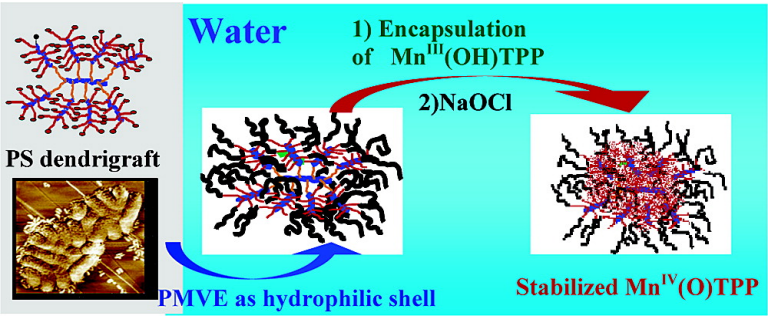

More About This Article

Additional resources and features associated with this article are available within the HTML version:

- Supporting Information
- Links to the 6 articles that cite this article, as of the time of this article download
- Access to high resolution figures
- Links to articles and content related to this article
- Copyright permission to reproduce figures and/or text from this article

View the Full Text HTML

J|A|C|S
ARTICLES
Published on Web 02/08/2005

Molecular Containers Based on Amphiphilic PS-*b*-PMVE Dendrigraft Copolymers: Topology, Organization, and Aqueous Solution Properties

Michel Schappacher,[†] Jean Luc Putaux,[‡] Christelle Lefebvre,[†] and Alain Deffieux*[,†]

Contribution from the Laboratoire de Chimie des Polymères Organiques, UMR 5629 ENSCPB-CNRS, Université Bordeaux 1,16 avenue Pey Berland, 33607 Pessac Cedex, France, Centre de Recherches sur les Macromolécules Végétales, ICMG-CNRS, Joseph Fourier University of Grenoble, BP 53, F-38041 Grenoble Cedex 9, France

Received October 1, 2004; E-mail: deffieux@enscpb.fr

Abstract: The synthesis, characteristics, and properties of amphipatic, water-soluble dendrigrafts, with a polystyrene core and polystyrene-*b*-poly(methyl vinyl ether) (PS-*b*-PMVE) diblock as external branches, are described. The dendrigrafts are observed by AFM and TEM as egglike or long cylindrical objects which can self-organize intramolecularly in segregated subdomains forming flowerlike or strings of flowerlike objects. In organic solvents the dendrigrafts behave as fully soluble isolated macromolecules and show in water a low critical solubility temperature (LCST) at $t > 30$ °C. The ability of the amphiphilic PS-*b*-PMVE dendrigrafts to complex and transport in water organic (pyrene) and metallo-organic (manganese tetraphenyl porphyrin) molecules is investigated. The possibility to stabilize the high oxidation state of metallo-porphyrin complexes through their encapsulation into the dendrigraft is shown.

Introduction

In recent years, important research activity has been devoted to the synthesis and study of branched and hyperbranched macromolecules with starlike, comblike, and dendritic architectures.[1−3] Dendrigrafts which belong to this last family are highly branched molecules characterized by several branching levels. We have recently reported a strategy of synthesis of such architectures based on the successive use of anionic and cationic living polymerizations for the preparation of the elementary macromolecular building bricks.[4] These successive construction steps can be exploited to build macromolecules constituted of macromolecular domains with distinct chemical composition. This strategy was recently applied to the preparation of dendrigrafts possessing external branches constituted of styrene and protected hydrophilic poly(vinyl ether) diblocks. After a deprotection step, water-soluble polystyrene-*b*-poly(hydroxyethylvinyl) ether (PS-*b*-PVEOH) dendrigrafts were obtained.[5] Since polystyrene and poly(vinyl ether) blocks are incompatible, they tend to self-organize intramolecularly, within the macromolecule, to form segregated subdomains yielding original morphologies such as the recently observed grapelike organization.[5] Such specific spatial arrangement in nanometer-size domains can be explained by the capacity of macromolecular blocks constituting a branch (polystyrene and poly(vinyl ether)) to get in contact and associate with the blocks of the same nature in neighboring branches, within the dendrigraft macromolecule. Their capacity to self-assemble and the subdomain size will depend on their relative proximity, block length, and limited degree of freedom, since each block copolymer branch is linked at one end to the dendrigraft backbone.

Continuing this work on the synthesis and properties study of amphipatic dendrigrafts, we have investigated the preparation of polystyrene dendrigrafts with polystyrene-*b*-poly(methyl vinyl ether) (Ps-*b*-PMVE) diblock as external branches, since the PMVE presents very interesting features. First it is the unique alkyl vinyl ether monomer for which living cationic polymerization directly yields a hydrophilic and water-soluble polymer, without the necessary use of any protection/deprotection steps.[3] Moreover PMVE chains exhibit in water a low critical solubility temperature (LCST) and shows dissolution/precipitation characteristics, at about 37 °C, that could be of great interest when associated to the already reported complexing ability of amphiphilic dendrigrafts toward organic and metal organic guest molecules. These characteristics could be valuably used, for instance, to complex or transport selectively compounds dispersed in water media and extract them by temperature raising.

The present paper reports on the synthesis of PS dendrigrafts with PS-*b*-PMVE external branches, their molecular characteristics, and solubility parameters. Their internal organization in

[†] Université Bordeaux 1.
[‡] Joseph Fourier University of Grenoble.

(1) (a) Branched Polymers I and II. *Advances in Polymer Science*; Roovers, J., Vol. Ed.; Springer-Verlag: Berlin, 1999; Vols. 142 and 143. (b) *Dendrimers and other Dendritic Polymers*, Frechet, J. M. J.; Tomalia, D. A.; Eds.; Wiley: Chichester, 2001.
(2) Star and hyperbranched Polymers. *Plastics Engineering Series*; Mishra, M. K., Kobayashi, S., Eds.: Marcel Decker, Inc.: New York, 1999; Vol. 53.
(3) Teertstra S. J.; Gauthier M. *Prog. Polym. Sci*. **2004**, *29*, 277.
(4) Muchtar, Z.; Schappacher, M.; Deffieux, A. *Macromolecules* **2001**, *34* (22), 7595−7600.
(5) Schappacher, M.; Deffieux, A.; Putaux, J.-L.; Viville, P.; Lazzaroni, R. *Macromolecules* **2003**, *36* (15), 5776−5783.

10.1021/ja0440203 CCC: $30.25

Scheme 1

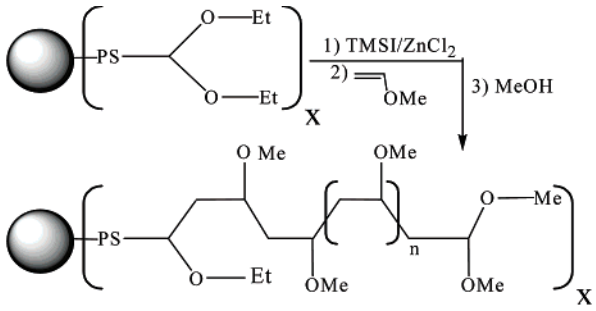

with **X,** the number of external branches in the range 10^4 **(1-PMVE)** to 10^5 **(2-PMVE)**

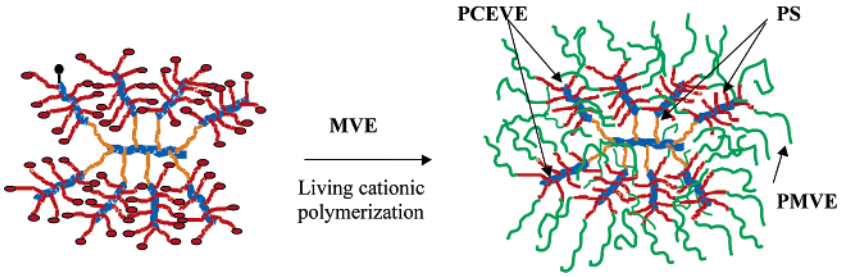

Table 1. Composition, Hydrodynamic Radius Rh in nm, and Polydispersity Index in Different Solvents of PS Dendrigafts with PS or PS-*b*-PMVE as External Branches

structure of external branches (ref)	composition (PCEVE-*g*(-PS-*b*-PCEVE-*g*-(**PS-*b*-PMVE**)))	Rh THF[d]	Rh MeOH[d]	Rh H_2O[d]
PS (1-PS)[a]	200-50-50-**50**	43 (*1.15*)[e]		
PS-*b*-PMVE (1-PMVE)	200-50-50-**50-360**[c]	75 (*1.20*)	63 (*1.26*)	60 (*1.16*)
PS (2-PS)[b]	1000-80-170-**70**	94 (*1.19*)		
PS-*b*-PMVE (2-PMVE)	1000-80-170-**70-165**[c]	120 (*1.34*)	97 (*1.32*)	92 (*1.33*)

[a] $M_w = 3.8 \times 10^7$ g/mol as determined by SLS in THF[5]; experimental number of external branches: 7600. [b] M_w was too high to be measured by SLS (non linearity of Debye plots). Estimation by calculation assuming quantitative PS grafting and CEVE polymerization reactions yields a theoretical value of about 1×10^9 g/mol and a number of external branches of 170 000 (1000×170) per dendrigraft. [c] $\overline{DP}_n$ of the different building blocks. [d] At $T = 25$ °C. [e] Values in parentheses are polydisperity indexes.

selective and nonselective organic solvents was also studied using atomic force microscopy and cryo-electron transmission microscopy. Finally, their complexation properties for extraction/transport purpose were investigated.

Experimental Section

Materials. Toluene (99,5%, J.T. Baker, Deventer, The Netherlands) was purified by distillation over calcium hydride and stored over polystyryllithium seeds. Diethyl ether (99%, J.T. Baker, Deventer, The Netherlands) was purified by distillation over calcium hydride and stored over potassium/benzophenone. Trimethylsilyl iodide (TMSI, Aldrich 97%) and $ZnCl_2$ (Aldrich 99,99%) were used without further purification. Gaseous methyl vinyl ether (MVE, Fluka Chemika 99%) was distilled over calcium hydride twice before use. 5,10,15,20-Tetraphenyl-21*H*,23*H*-porphine manganese(III) chloride (MnClTPP) (99%, Sigma-Aldrich France) and pyrene (98%, Sigma-Aldrich France) were used as received. Sodium hypochlorite (NaOCl) (Sigma-Aldrich, solution 10−13% available chlorine) was also used as such.

Synthesis of the PS Dendrigraft Precursors. The dendrigraft precursors, (**1-PS**) 200/50/50/50-A ($\overline{DP}_{n\text{PCEVE1}}/\overline{DP}_{n\text{PS1}}/\overline{DP}_{n\text{PCEVE2}}/\overline{DP}_{n\text{A-PS2}}$, A = α-diethylacetal) and (**2-PS**) 1000/80/170/70-A, used in this work were elaborated according to a previously reported procedure[6] (Scheme 1). The absence of ungrafted PS was checked by SEC. The dimensions of these hyperbranched polymers are collected in Table 1.

Synthesis of Amphipatic PS Dendrigrafts with an Hydrophilic PMVE Shell (1-PMVE and 2-PMVE). The dendrigrafts were prepared as previously described[6] by initiation of living cationic polymerization of methyl vinyl ether from the diethylacetal ends of external PS branches of the hyper-branched PS cores. A typical sequential polymerization procedure was as follows: 5 g of dendrigraft (**1-PS**) (corresponding to 1 mmol of diethyl acetal ends) and 200 μL (1.4 mmol) of TMSI were added successively to 150 mL of dry toluene under vacuum at −35 °C. After 45 min, 23.2 g (0.4 mol) of MVE were added, and the polymerization was started by addition of 13 mg of $ZnCl_2$ (0.1 mmol) dissolved in 1.5 mL of diethyl ether. Every 2 h a small sample of the reaction mixture was taken for characterization purpose, and the MVE conversion was followed by SEC analysis. After complete MVE conversion (6 h), a lutidine/methanol solution (10% v/v) was added to deactivate the system. The reaction mixture was washed with 10% aqueous sodium thiosulfate solution and water and dried over $MgSO_4$ and then under vacuum (yield 18.5 g). Linear PMVE which forms as side product was removed by selective fractionation. Complete removal was confirmed by SEC. The average PMVE block length was calculated by ^1H NMR from the proportion between MVE and styrene units in the copolymer, assuming quantitative initiation from all the PS acetal ends.

Preparation of PS−PMVE Dendrigraft Aqueous Solutions. For studies in water, 10 g of dendrigraft **1-PMVE** were dissolved in 50

(6) (a) Deffieux, A.; Schappacher, M. *Macromolecules* **1999**, *32*, 1797−1802. (b) Deffieux, A.; Schappacher, M. *Macromolecules* **2000**, *33*, 7371−7377. (c) Schappacher, M.; Billaud, C.; Paulo, C.; Deffieux, A. *Makromol. Chem. Phys.* **1999**, *200*, 2377−2386.

mL of ethanol and purified and transferred into water by dialysis (Spectra/Por7, molecular weight cutoff ca. 1000) for 3 days against pure water at 20 °C.

Atomic Force Microscopy (AFM). Samples for AFM analysis were prepared by solvent casting at ambient conditions by spin coating on substrates starting from solutions in dichloromethane for the polystyrene core dendrigraft or methanol and water for the PMVE derivated dendrigrafts. Practically, 20 μL of a dilute solution (0.01 wt %) were spin cast on a 1 × 1 cm^2 freshly cleaved mica or on a highly oriented pyrolytic graphite (HOPG) substrate. Samples were analyzed after complete evaporation of the solvent at room temperature. All AFM images were recorded in air with a Dimension microscope (Digital Instruments, Santa Barbara, CA), operated in tapping mode. The probes were commercially available silicon tips with a spring constant of 40 N/m, a resonance frequency lying in the 270−320 kHz range, and a radius of curvature in the 10−15 nm range. In this work, both the topography and the phase signal images were recorded with the highest sampling resolution available, i.e., 512 × 512 data points.

Transmission Electron Microscopy (TEM). Droplets of 0.01 mg/mL dendrigraft solutions were deposited onto carbon-coated microscopy grids. To limit the reconcentration resulting from the fast evaporation of organic solvents, the liquid in excess was immediately blotted with filter paper. A droplet of aqueous uranyl acetate (2 wt %) was deposited onto the specimen before drying. The excess of stain was blotted, and the remaining liquid film was allowed to dry. As uranyl acetate is known not to dissolve into organic solvents, our concern was that salt recrystallization artifacts would appear when the aqueous solution was in contact with the residual film of organic solvent. Surprisingly, as shown in the Results section, negative staining worked well using this method.

Cryo-TEM has been successfully used to observe various polymer nanoparticles dispersed in water,[7,8] but there exists very few examples of systems in organic solvents that were studied with this technique.[9−11] The main reason is that most organic solvents are known to dissolve in liquid ethane which is the cryogen commonly used for fast-freezing. Thus, organic solvents have to be quench-frozen in liquid nitrogen. However, due to a low freezing efficiency, the resulting film is often crystalline, and that creates detrimental diffraction effects during TEM observation.

In the present study, two organic solvents were used: methanol and dichloromethane. Thin films of 1 mg/mL dendrigraft suspension in methanol were formed on NetMesh (Pelco) "lacey" carbon membranes and immediately plunged into liquid ethane (−171 °C) using a Leica EM CPC fast-freezing device.[8] As checked by cryo-TEM, methanol was successfully vitrified using liquid ethane. Dendrigraft suspensions in dichloromethane had to be quenched in liquid nitrogen, using a homemade guillotine-type plunging system and a glass Dewar containing the cryogen. The specimens were then mounted onto a Gatan 626 cryo-holder cooled with liquid nitrogen and transferred into the microscope. All samples were observed at −180 °C using a Philips CM200 "Cryo" microscope operated at 80 kV. One major problem was that vitreous solvents appeared to be highly radiation sensitive. Bubbles rapidly developed under electron irradiation. The only way to record images at magnifications of 15 000−30 000× was to use the Low Dose System (FEI/Philips): the region of interest was chosen at low magnification and low illumination while focusing was performed at a higher magnification on an area nearby. Micrographs were recorded on Kodak SO163 films.

Dynamic Light Scattering (DLS). Light scattering measurements were performed using an ALV laser goniometer, which consists of a 22 mW HeNe linear polarized laser with 632.8 nm wavelength and an ALV-5000/EPP multiple τ digital correlator with 125 ns initial sampling time. Solutions were put in 10 mm diameter glass cells and kept at a constant temperature of 25 °C. Scattering measurements were done from 30° to 130 or 150° with a step of 20° or from 30° to 120° with a step of 30°: only data at 90 °C are presented. The data acquisition was done with ALV correlator control software, and the counting time varied for each sample from 300 up to 600 s.

Other Characterization Techniques and Measurements. ^{1}H NMR spectra were recorded in $CDCl_3$ on a Bruker Avance 400 MHz FT apparatus. Size exclusion chromatography (SEC) analysis in THF (distilled from CaH_2) was performed at 25 °C at a flow rate of 0.7 mL/min on a Varian apparatus equipped with refractive index/laser light scattering (Wyatt technology) dual detection and fitted with four TSK columns (300 × 7.7 mm^2, 250 Å, 1500 Å, 10^4 Å, 10^5 Å). UV−vis spectroscopy measurements were performed at 20 °C on a Varian Cary measurements 3E apparatus in UV quartz cells of 5 mm. Fluorescence spectra were recorded on a Safas Monaco FLX spectrofluorometer at 310 nm excitation wavelength at room temperature.

Preparation and Study of Pyrene/PS−PMVE Dendrigraft Complexes. Pyrene (4.7 mg, 2.3 × 10^{-6} mol) was first dissolved in 0.5 mL of dichloromethane in a small flask, and the solvent was evaporated until dryness. A solution of PS−PMVE dendrigraft (**1-PMVE**) (20 mL 1.3 mg/mL, 1.7 × 10^{-10} mol) in pure water (milli-Q) was then added under vigorous stirring at 20 °C, and the UV−visible absorption spectra of the water solution was recorded at increasing time.

Preparation and UV−visible Study of Metalloporphyrin/PS−PMVE Dendrigraft Complexes. The metalloporphyrin (Mn^{III}ClTPP) (1.7 mg as fine powder, 2.4 × 10^{-6} mol) was poured into the pure water (milli-Q) solution of PS−PMVE dendrigraft (**1-PMVE**) (30 mL 1.3 mg/mL, 2.5 × 10^{-10} mol) at 20 °C, pH = 7 under vigorous stirring. The UV−visible absorption spectra were recorded at increasing time until the intensity of the absorption spectra remained constant (12 h) indicating complete encapsulation.

Oxidation of Dendrigraft Complexed Mn^{III}ClTPP with Sodium Hypochlorite: Generation of Oxo-Mn^{IV}TPP. In a quartz cuvette (5 mm optical path) containing an aqueous solution of Mn^{III}ClTPP/dendrigraft (**1-PMVE**) (0.17 mg of Mn^{III}ClTPP in 3.9 mg of **1-PMVE** in 3 mL water, pH 7, 20 °C) was introduced in small portions a water solution of sodium hypochlorite (1 μL aliquots of a 1% solution), and the UV−visible spectrum of the solution was monitored with time. The resulting visible spectrum (λ_{max}(nm) = 424, 473, 520, 625) is characteristic of red oxo-Mn^{IV}TPP complex. Stability of the Mn^{IV}/**1-PMVE** complex versus time was then followed by the intensity decrease of the characteristic absorption bands with time.

Results and Discussion

The synthetic pathway used for the synthesis of dendrigrafts with a PS core and PS-*b*-PMVE external branches is directly derived from the previously reported synthesis and purification of polystyrene-*b*-poly(vinyl ether) dendrigrafts. PMVE blocks were introduced by initiation of MVE cationic polymerization from a PS dendrigraft bearing an acetal function terminus at each of its external PS branches (Scheme 1). Initiation from this multifunctional precursor requires the preliminary transformation of the acetal end group into an α-iodoether by addition of trimethylsilyl iodide (TMSI). Propagation is then triggered by adding zinc dichloride as catalyst and the monomer. In agreement with previous data[5] the efficiency of the initiation reaction was estimated by proton NMR higher than 90%. The very high increase of molar mass at each dendrigraft building step allowed an easy fractionation of the dendrigrafts from the linear PMVE homopolymers by selective precipitation.

(7) Chalaye, S.; Bourgeat-Lami, E.; Putaux, J. L.; Lang, J. *Macromol. Symp.* **2001**, *169*, 89−96.
(8) Durrieu, V.; Gandini, A.; Belgacem, M. N.; Blayo, A.; Eiselé, G.; Putaux, J. L. *J. Appl. Polym. Sci.* **2004**, *94−2*, 700−710.
(9) Oostergetel, G. T.; Esselink, F. J.; Hadziioannou, G. *Langmuir* **1995**, *11*, 3721−3724.
(10) Boettcher, C.; Schade, B.; Fuhrhop, J. H. *Langmuir* **2001**, *17-3*, 873−877.
(11) Butter, K.; Bomans, P. H.; Frederik, P. M.; Vroege, G. J.; Philipse, A. P. *Nature Materials* **2003**, *2-2*, 88−91.

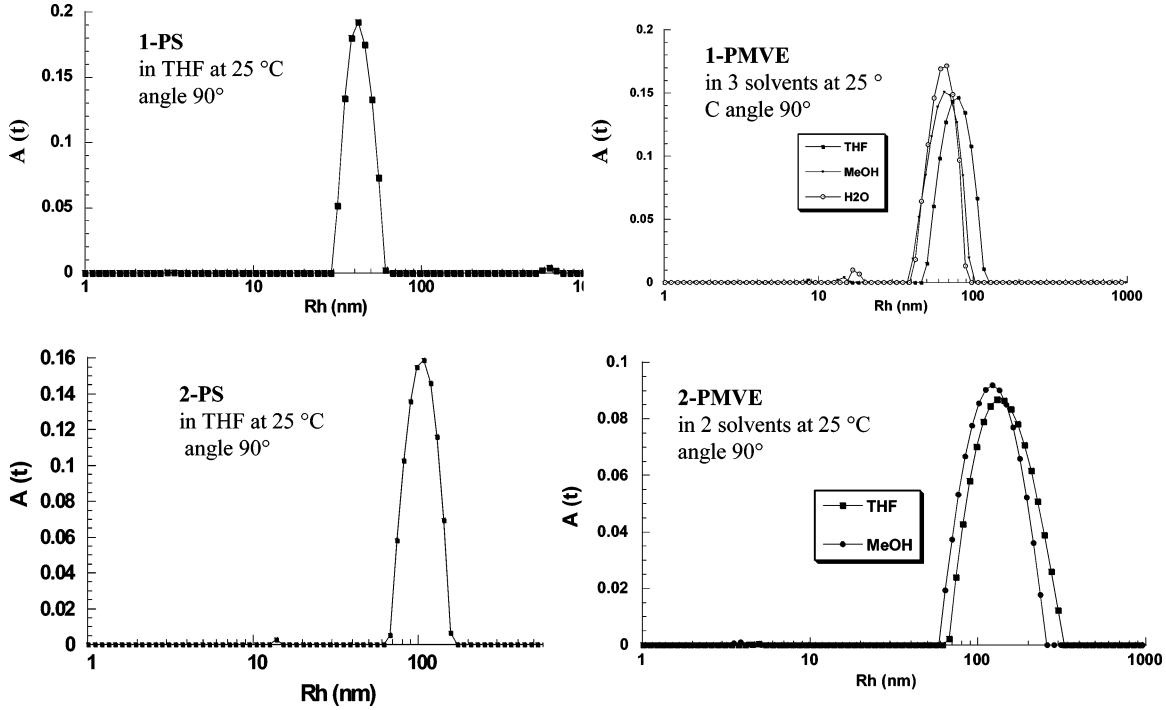

Figure 1. Hydrodynamic radius and polydispersity of PS and PS-*b*-PMVE dendrigrafts in different solvents as determined by DLS.

The architectural characteristics of the initial PS dendrigrafts **1-PS** and **2-PS** and final PS-*b*-PMVE amphiphilic dendrigrafts **1-PMVE** and **2-PMVE** and their dimensional parameters in different solvents are collected in Table 1.

Good solubility of PS and PS-*b*-PMVE dendrigrafts is observed in THF and dichloromethane which are solvents of both PS and PMVE blocks. DLS measurements performed at various angles (30° to 120°) indicates the presence of a single population for dendrigrafts **1-PMVE** and **2-PMVE**. As indicated by their hydrodynamic radius and narrow size distribution in solution, the hyperbranched macromolecules (Figure 1) behave as isolated molecules without any detectable formation of intermolecular aggregates. The important increase of the hydrodynamic radius in THF after MVE polymerization, comparing **1-PS** with **1-PMVE** and **2-PS** with **2-PMVE**, Table 1, confirms the important growth of the macromolecule due to the formation of the PMVE shell. The PS−PMVE core−shell-like macromolecules are also soluble in methanol and water (at $T < 25$ °C), which are selective solvents of the PMVE shell. As it may be noticed in Table 1, a strong reduction of the hydrodynamic radius of the PS−PMVE dendrigrafts is observed in these solvents as compared to THF. This can be explained by the internal contraction of the PS core in methanol and water nonsolvents. However, the influence of changes in solvent quality for the PMVE material may also contribute to this phenomenum. Although the PS-*b*-PMVE dendrigrafts exhibit a much more compact PS core, thanks to the PMVE shell they remain soluble and behave as monodisperse unimolecular objects, as indicated by DLS data Figure 1. This can be related to the highly protecting effect of the PMVE shell which limits dendrigraft−dendrigraft associations through interaction between their PS core.

In methanol, the PS−PMVE dendrigrafts exhibit very similar characteristics and behavior (almost same size and polydispersity, no aggregation) in the whole temperature range examined, whereas a strong influence of temperature is observed in water

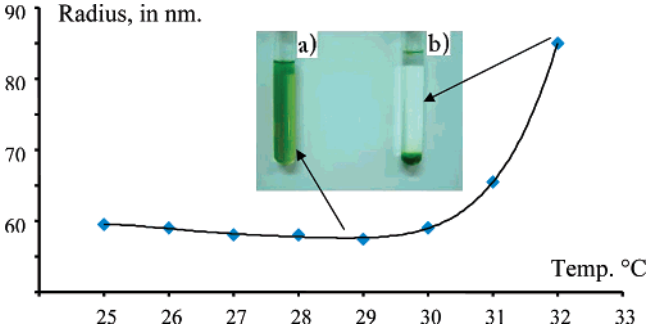

Figure 2. Variation of the hydrodynamic radius of PS-*b*-PMVE dendrigraft (**1-PMVE**) in water as a function of temperature (60 min between two measurements). Inset: aqueous solution of (Mn^{III}TPP)OH in dendrigraft (**1-PMVE**): (a) at 20 °C; (b) after raising the temperature at 35 °C for 60 min. Dendrigraft (**1-PMVE**) concentration: $\sim 1 \times 10^{-8}$ M; (Mn^{III} TPP)Cl $\approx 1.10^{-4}$ M

solutions. The average hydrodynamic radius of dendrigrafts **1-PMVE** as a function of the temperature is shown in Figure 2. A small decrease of the hydrodynamic radius at temperatures ranging from 25 to 30 °C is first observed. This can be related to a volume contraction of the PMVE shell associated to its solubility decrease when temperature increases. This phenomenon is followed at 30 °C by a rapid increase of the apparent hydrodynamic radius and a size distribution broadening of the objects, suggesting aggregation between dendrigraft molecules prior their precipitation. This is in agreement with the LCST properties brought by the PMVE shell to the dendrigraft.[12,13] However, contrarily to the reversibility of LCST processes reported for linear homo- and block PMVE copolymers, the solubilization/precipitation process is not reversible with the dendrigrafts. Considering that water is not a particularly good solvent for that polymer, this is likely due to strong intra- and

(12) Verdonck, B.; Goethals, E. J.; Prez, F. E. D. *Macromol. Chem. Phys.* **2003**, *204* (17), 2090−2098.
(13) Folder, C.; Patrickios, C. S.; Armes, S. P.; Billingham, N. C. *Macromolecules* **1996**, *29*, 8160−8169.

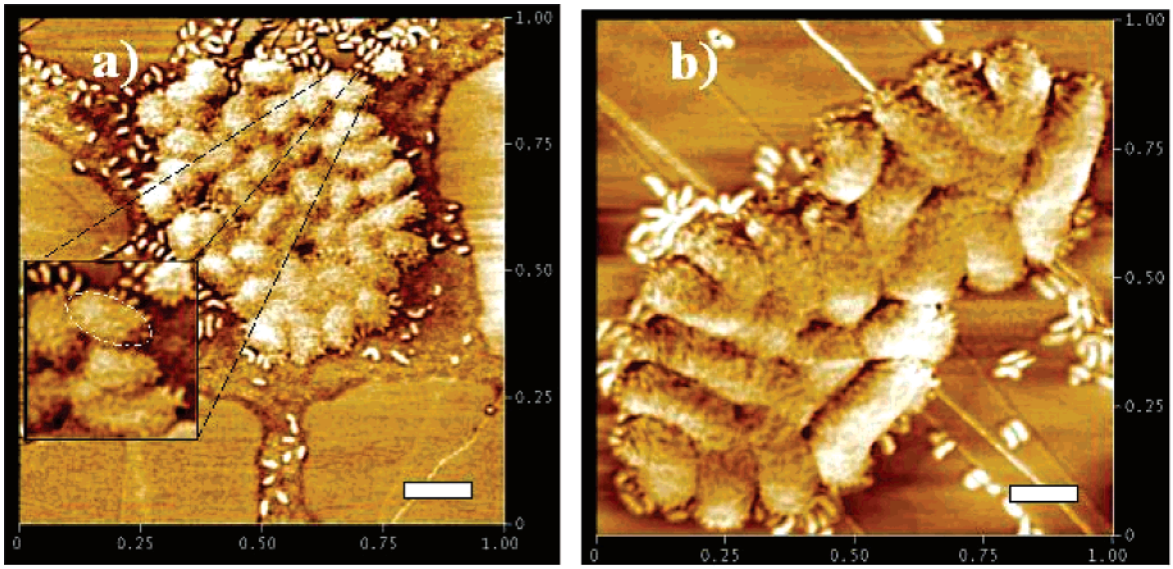

Figure 3. TMAFM images of PS dendrigrafts deposited from dichloromethane solutions: (a) **1-PS** (phase: $1 \times 1\ \mu$m); (b) **2-PS** (phase: $1 \times 1\ \mu$m). Scale bars: 100 nm.

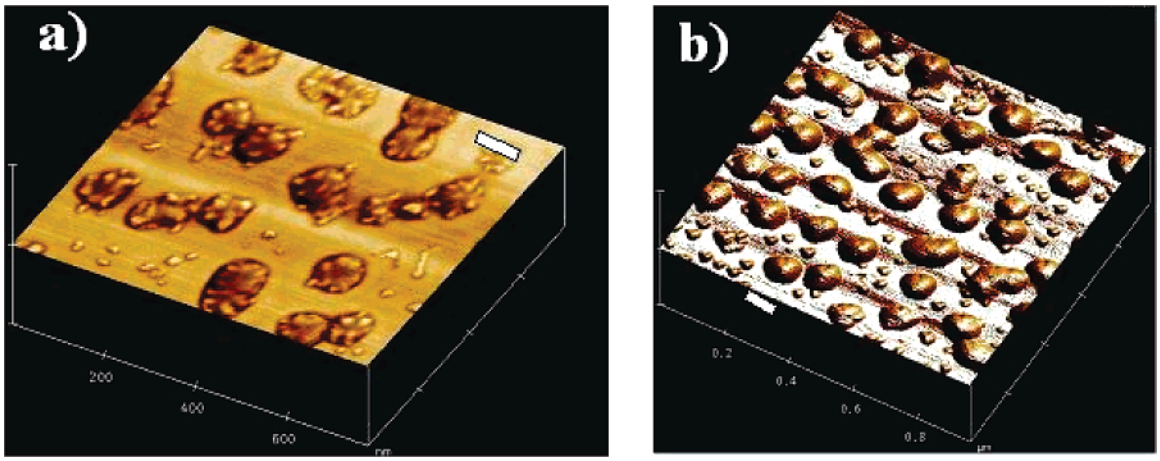

Figure 4. TMAFM phase images of PS-*b*-PMVE dendrigraft (**1-PMVE**) deposited from (a) methanol (750×750 nm^2) and (b) water (1000×1000 nm^2). The ratio of "tapping" amplitude to "free" cantilever oscillation amplitude was equal to 0.7 for image a and 0.95 for image b.

intermolecular associations yielding intermolecular entanglements between PMVE blocks. A similar temperature dependence was observed also with **2-PMVE**, although temperatures of the different phenomena were slightly lower due to the difference in the dendrigraft chemical composition, molar masses, and possibly their shape.

The shape and internal organization of the dendrigrafts were further examined in the solid using AFM and TEM. AFM images obtained from dichloromethane solution deposits of PS dendrigrafts **1-PS** and **2-PS**, corresponding to the hydrophobic core of the PS−PMVE amphiphilic dendrigrafts, are shown in Figure 3. They appear as monolayer aggregates of uniform objects which sizes (75×50 nm^2 and 300×100 nm^2, respectively) in good agreement with the dimensions of the different building blocks. Their specific shape, egglike for **1-PS** and cylindrical for **2-PS**, is determined by the ratio between their length and cross section. The length is mainly governed by the $\overline{DP}_n$ of the central poly(chloroethyl vinyl ether) (PCEVE) backbone ($\overline{DP}_{nPCEVE1}$ 200 and 1000, respectively), whereas the other constitutive blocks PS_1, $PCEVE_2$, PS_2, contribute to the cross section of the objects. In the case of **1-PS** and **2-PS**, the presence of smaller objects attributed to dendrigraft fragments can also be noticed. AFM images of PS-*b*-PMVE dendrigrafts (**1-PMVE**) were obtained from deposits of their methanol and water solutions, after drying. Images obtained from THF deposits show spherical objects similar to those presented in Figure 3a but with a larger diameter of 100 nm, in agreement with the formation of the PMVE blocks. Those obtained from methanol deposits, a nonsolvent of the PS core, exhibit a quite different structure with a specific intramolecular organization (Figure 4a) corresponding to hard and soft subdomains of different chemical composition, as previously reported for other amphiphilic dendrigrafts.[5] The image obtained from aqueous deposits does not show any specific internal organization (Figure 4b). This may be explained by the presence of remaining water inside the dendrigrafts which does not allow us to distinguish hard and soft phases.

Figure 5 shows TEM micrographs of dendrigraft preparations after negative staining. Dendrigrafts **1-PMVE** appear as ovoid particles with a width of 80−100 nm and a length of 100−120 nm (Figure 5a). Their multilobular aspect is similar to that of previously studied dendrigrafts dispersed in water.[5] We have

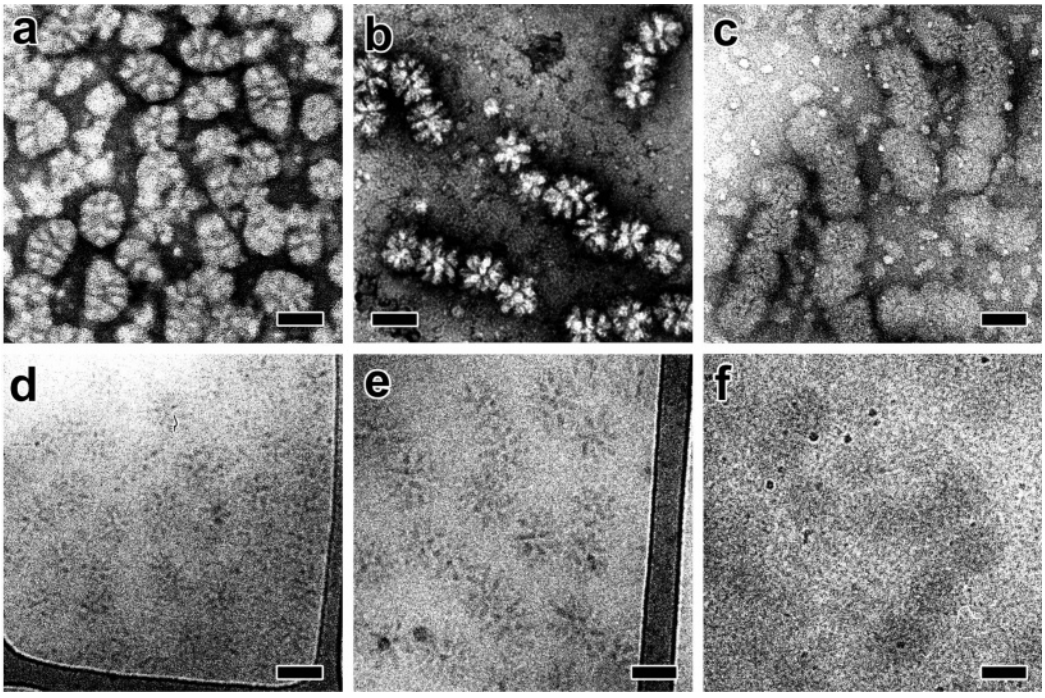

Figure 5. TEM images of dendrigrafts from samples **1-PMVE** and **2-PMVE** suspended in methanol (a,d and b,e, respectively) as well as sample **2-PMVE** suspended in dichloromethane (c,f). In images a−c, the dry specimens were negatively stained with uranyl acetate, whereas, in images d−f, the dendrigrafts are seen embedded in thin films of vitrified methanol (b,e) and dichloromethane (f). Scale bars: 100 nm.

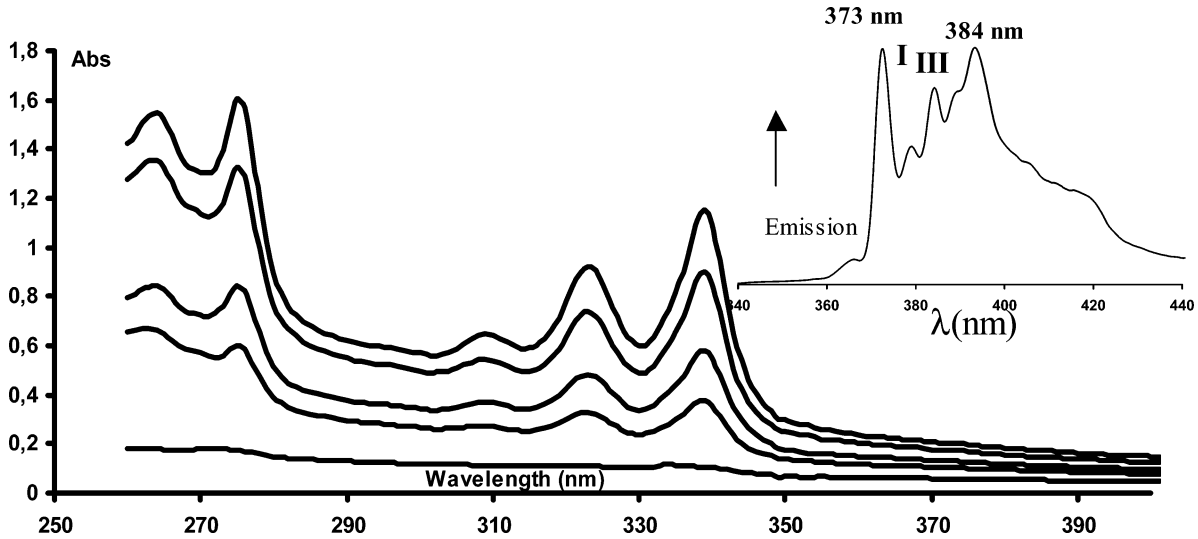

Figure 6. Evolution of the UV−visible spectrum of a pyrene (1.15×10^{-4} M)/dendrigraft (**1-PMVE**) (8.5×10^{-9} M) mixture in water at increasing contact time: (a) 1 min; (b−j) 15, 30, 105, 180, 300, 1320 min. Inset: fluorescence spectrum emission ($\lambda_{\text{excitation}} = 310$ nm) of pyrene/dendrigraft in water.

shown that this peculiar morphology was not the result of a drying artifact but was indeed related to the reorganization of hydrophobic PS branches into chemically distinct subdomains. These domains are formed by the intramolecular aggregation between nonmiscible hydrophilic PMVE (soft phase) on one hand and hydrophobic PS blocks (hard phase) on the other hand, the volume fraction of PCEVE anchoring sites being negligible. Since PS and PMVE are miscible in the bulk, the segregation process likely takes place in the methanol solution used for the sample preparation.

Negatively stained dendrigrafts (**2-PMVE**) built on a longer PCEVE backbone and dispersed in methanol appear as strings of flowerlike particles with a 100 nm diameter (Figure 5b), similar to individual dendrigrafts (**1-PMVE**). This suggests that the main central PCEVE backbone breaks into smaller units, although these units could not clearly be seen as individual objects. Dendrigrafts **2-PMVE** suspended in dichloromethane, in which all types of branches are soluble, were also observed after negative staining. As seen in Figure 5c, the flowerlike morphology has disappeared in agreement with the fact that the macromolecules are fully swollen in dichloromethane and that no chemical segregation is detected. The dendrigrafts also appear as strings of 100 nm spheroid subunits which confirm the fragmentation of the central PCEVE backbone observed in methanol. Surprisingly, these 100 nm units were not detected either by SEC or DLS. It is thus difficult to know if the fragmentation took place during the synthesis, the storage in solution, or the sample preparation for imaging where the

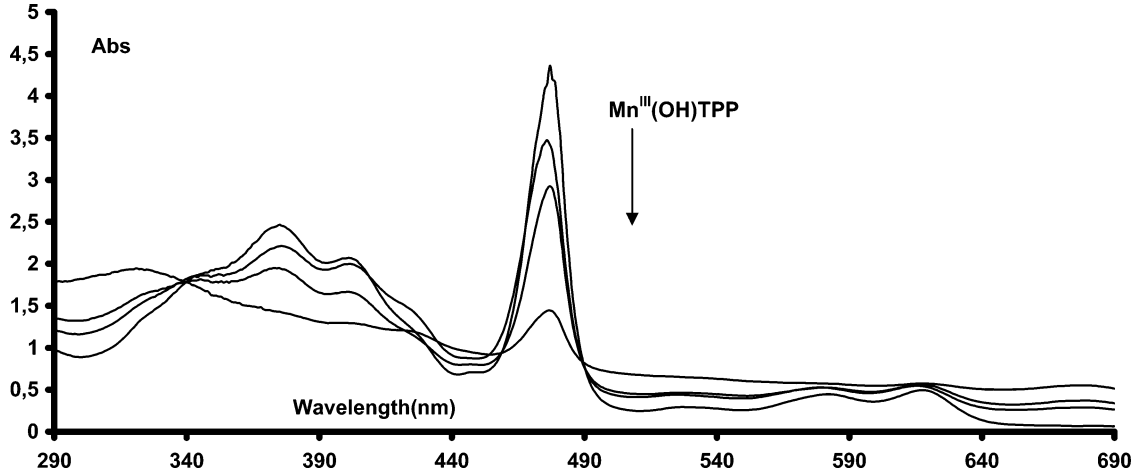

Figure 7. Kinetics of decomposition of $Mn^{III}ClTPP$ in dichloromethane in the presence of NaOCl monitored by UV−visible absorption spectroscopy at 20 °C (10 min between two scans). $[Mn^{III}ClTPP] = 1.1 \times 10^{-5}$

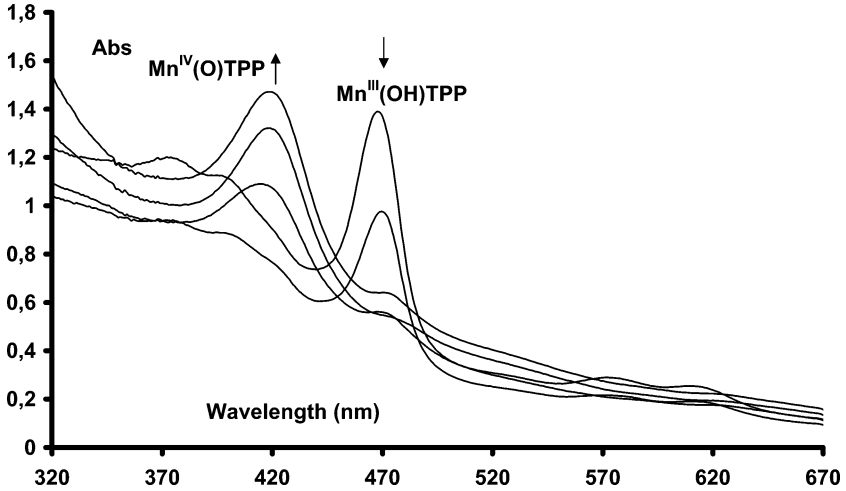

Figure 8. UV−visible absorption spectrum in water of $Mn^{III}(OH)TPP$ (formed from MnClTPP) encapsulated into PS-*b*-PMVE dendrigrafts before and after addition of several aliquots of NaOCl at 20 °C. $[MnClTPP] = 1.1 \times 10^{-5}$ M

molecules may be submitted to important mechanical constraints associated to their overcrowded structures and the phase segregation process.

Samples **1-PMVE** and **2-PMVE** were also observed using cryo-TEM. Figure 5d and e show images of dendrigrafts embedded in vitreous methanol (fast-freezing in liquid ethane). The contrast in this organic solvent is clearly lower than that of particles previously observed in vitreous ice.[5] Moreover, while defocus values of 1−3 μm are usually chosen for cryo-TEM imaging, we used higher defoci (4−6 μm) in order to enhance the phase contrast and reveal the particles. In the resulting images, only the denser parts, which likely correspond to subdomains of insoluble PS branches, are detected, whereas the PMVE corona is too diffuse to be seen. When sample **2-PMVE** is observed in vitreous dichloromethane (frozen in liquid nitrogen), only a weak amplitude contrast is detected on the particles (Figure 5f). This confirms that the branches are soluble and that the dendrigrafts are fully swollen in this solvent. However, the cryo-TEM images of sample **2-PMVE** suspended in methanol or dichloromethane confirm that the peculiar morphology observed on negatively stained specimens was not a drying artifact. In both cases, the dendrigrafts appear as strings of 100 nm units, suggesting that the fragmentation occurred in an earlier preparation step.

The capacity of amphipatic PS−PMVE dendrigrafts to solubilize and transport into water small organic molecules and organometallic complexes (pyrene and manganese(III) tetraphenyl porphyrin, $Mn^{III}(X)TPP$, were chosen as models) has been investigated in aqueous media. Solid pyrene (1.15×10^{-4} M) was contacted with an aqueous solution of **1-PMVE** (8.5×10^{-9} M), and the turbid mixture was maintained under stirring at 20 °C until it turned to an homogeneous colorless solution. The evolution of the absorption spectrum of the pyrene/dendrigraft mixture at increasing contact time (Figure 6) confirms the transportation of pyrene into water through its complexation by **1-PMVE**. The characteristics of the pyrene absorption bands in the water/dendrigraft system (λ_{max}(nm) = 263, 275, 297, 309, 323, 339) are very close to those observed in conventional organic solvents (λ_{max}(nm) = 262, 274, 295, 307, 321, 337 in dichloromethane). According to the UV−visible spectroscopy, at completion about 13 500 molecules of pyrene are contained in one molecule of dendrigraft.

Under UV light irradiation (λ = 365 nm), the pyrene/dendrigaft aqueous solution exhibits a fluorescent blue emission very similar to that of pyrene in organic solvent. The fluorescence spectrum (inset in Figure 6) shows an intensity ratio I_{III}/I_I of about 0.85, a value much higher than generally reported for pyrene in water ($I_{III}/I_I = 0.59$) and polar media and in the

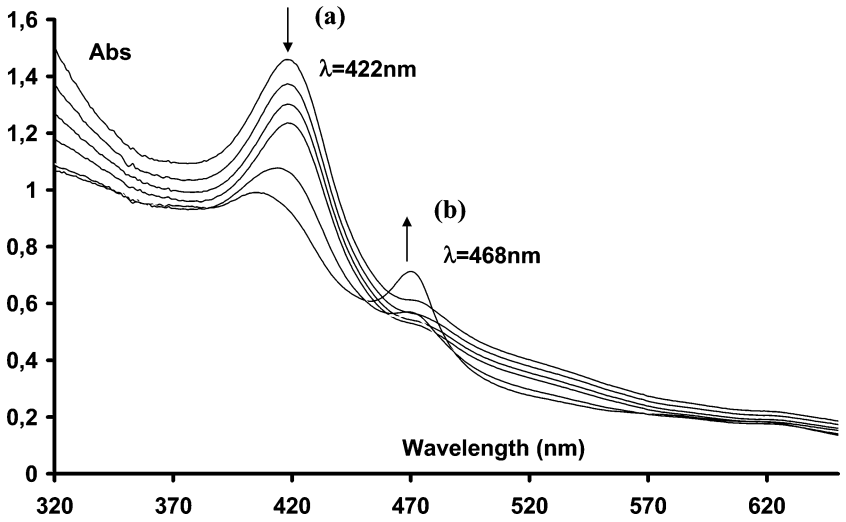

Figure 9. Kinetics of decomposition in water at 20 °C of Mn^{IV}oxoTPP encapsulated into PS-*b*-PMVE dendrigrafts as monitored by UV−visible absorption spectroscopy (20 min between two scans).

range of the fluorescence spectrum of pyrene in aromatic solvents ($I_{III}/I_I = 0.82$ to 1.0).[15] These observations suggest that the pyrene molecules captured in the dendrigraft are located within the polystyrene core and behave as individual molecules such as in an organic solution, despite the surrounding water medium and the high number of pyrene molecules per dendrigraft.

Complexation and transport of large metallo-organic molecules into water was investigated in the same way using manganese tetraphenylporphyrin chloride, (Mn^{III}TPP)Cl, as starting molecule. As shown by the homogeneous green-colored solution, the metalloporphyrin ($\sim 1 \times 10^{-4}$ M), added to the water solution of the PS−PMVE dendrigraft ($\sim 1 \times 10^{-8}$ M) as a fine powder, completely dissolves in less than 12 h at 20 °C (see inset a, Figure 2). The observed absorption bands are characteristic of (Mn^{III}TPP)OH ($\lambda_{max} = 468$ nm) which forms by hydrolysis of the chloride derivative when in contact with water. Interestingly, due to the LCST properties of the PMVE dendrigraft shell upon raising the temperature of the solution at about 35 °C, the metalloporphyrin/dendrigraft complex precipitates yielding a colorless solution (inset Figure 2) free of metalloporphyrin. This supports the fact that all the metalloporphyrin molecules are strongly trapped inside the dendrigrafts and can be easily and efficiently removed from water through this simple temperature-controlled precipitation process. As indicated before, resolubilization of the dendrigrafts at lower temperature was not possible.

Oxidized synthetic metalloporphyrin complexes have been extensively studied as simple active site models for monooxygenase[15] and peroxidase[16,17] as well as catalysts for the epoxidation reactions of organic substrates.[19,20] Indeed, structurally characterized oxometalloporphyrins of manganese, iron, and chromium are known for their unusual high reactivity in oxygen activation and transfer[11] and their ability to oxidize organic substrates. However, during these reactions, the metalloporphyrins act also frequently as a substrate for the oxidant and mutually destroy in an intermolecular process. This is illustrated in Figure 7 for Mn^{III}Cl TPP: addition of a small amount of NaOCl as oxidizing agent results in a very rapid disappearance of Mn^{III}Cl TPP without any observable formation of the oxidized Mn^{IV}OTPP derivatives. To enhance the metalloporphyrin stability toward oxidant, it is necessary to introduce bulky substituents on their phenyl and pyrrole groups. We found that dendrigraft encapsulated Mn^{III}OH TPP can be oxidized to yield relatively stable Mn^{IV} TPP species. As shown in Figure 8, upon addition of the oxidizing agent the main absorption band of encapsulated Mn^{III}(OH)TPP ($\lambda_{max} = 468$ nm) disappears to the benefit of a new soret band ($\lambda = 426$ nm) corresponding to the formation of Mn^{IV}oxoTPP species[16,21,22] which remains stable during several hours. The half-life time of dendrigraft complexed (Mn^{IV}TPP)oxo can be estimated from the half decay time of its soret band to 5 h at 20 °C (Figure 9). Since the main decomposition mechanism of the porphyrin ring in the oxidation process is believed to proceed via a bimolecular reaction, the strong stabilization effect observed with dendrigraft complexed (Mn^{IV}TPP)oxo suggests that the metalloporphyrins are isolated from each other inside the PS-*b*-PMVE dendrigraft, despite more than 10 000 molecules can be contained in one dendrigraft molecule. This could indicate that the metalloporphyrins are individually trapped in small and nonconnected cavities (of about 10 nm^3) delimited by the polystyrene chains. The location of (Mn^{IV}TPP)oxo molecules within the dendrigraft PS core is further supported by the independence of the oxo complex stability toward the pH of the solution from 7 to 14, contrarily to tetra(4-sulfonatophenyl) porphinato manganese(IV) X)/water systems[15] which show a stability increase toward NaOCl at increasing pH.

(14) Schappacher, M.; Deffieux, A. *Polymer* **2004**, *45*, 4633−4639.
(15) Collman, J. P.; Gagne, R. R.; Gray, H. B.; Hare, J. *J. Am. Chem. Soc.* **1974**, *96*, 6522.
(16) Groves, J. T.; Stern, M. K. *J. Am. Chem. Soc.* **1988**, *110*, 8628−8638.
(17) Liu, M.; Su, Y. O. *J. Electroanal. Chem.* **1997**, *426*, 197−203.
(18) Benaglia, M.; Danell, T.; Fabris, F.; Sperandio, D.; Pozzi, G. *Org. Lett.* **2002**, *24*, 4229−4232.
(19) Magno, S. G. D.; Dussault, P. H.; Schultz, J. A. *J. Am. Chem. Soc.* **1996**, *118*, 5312−5313.
(20) Davoros, E. M.; Diaper, R.; Dervissi, A.; Tornaritis, M. J.; Coutsocelos, G. *J. Porphyrins Phthalocyanines* **1998**, *2*, 53−60.
(21) Groves, J. T.; Watanabe, Y.; McMurry, T. J. *J. Am. Chem. Soc.* **1983**, *105*, 4489−4490.
(22) Schappacher, M.; Weiss, R. *Inorg. Chem.* **1987**, *26*, 1190−1192.
(23) Turk, H.; Berber, H. *Int. J. Chem.* **2000**, *32*, 271−278.
(24) Kalyanasundaram, K.; Thomas, J. K. *J. Am. Chem. Soc.* **1977**, *99*, 2039−2044.

The use of dendrigraft-stabilized oxidized manganese porphyrin complexes as potential catalysts for oxygen activation and transfer as well as for the oxidation of organic substrates will be further investigated. The preparation of stable oxidized forms of other metalloorganic complexes through dendrigraft encapsulation is also in progress.

JA0440203